

# Federated Client Selection under Partial Visibility: A POMDP Approach with Spatio-Temporal Attention

Qijun Hou<sup>1</sup>, Yuchen Shi<sup>1</sup>, Pingyi Fan<sup>1</sup> and Khaled B. Letaief<sup>2</sup>

<sup>1</sup>Dept. of Electronic Engineering, BNRist, Tsinghua University

<sup>2</sup>Dept. of Electronic and Computer Engineering, HKUST

{hqj23, shiyc21}@mails.tsinghua.edu.cn, fpy@mail.tsinghua.edu.cn, eekhaled@ust.hk

## Abstract

Federated learning relies on effective client selection to alleviate the performance degradation caused by data heterogeneity. Most existing methods assume full visibility of all clients at each communication round. However, in large-scale or edge-based deployments, the server can only access a subset of clients due to communication, mobility, or availability constraints, resulting in partial visibility where only a subset of clients is observable for aggregation in each communication round. In this paper, we formulate federated client selection under partial visibility as a Partially Observable Markov Decision Process (POMDP) and propose a Spatial-Temporal attention-based reinforcement learning framework. By integrating historical global models and client identity embeddings, the proposed method captures both the temporal contexts of training and the persistent characteristics of clients. Experimental results across multiple datasets demonstrate that our approach achieves superior performance compared to existing baselines in heterogeneous and partially visible settings, validating its effectiveness in addressing the challenges of incomplete observations in practical federated learning systems.

## 1 Introduction

Federated Learning (FL) enables collaborative model training across a large number of distributed clients while preserving data privacy. A fundamental challenge in FL arises from data heterogeneity, where client data distributions are non-independent identically distributed (non-IID), which significantly hinders model convergence and generalization. To address this issue, a large body of prior work has investigated advanced aggregation strategies and client selection mechanisms to better cope with non-IID data.

In addition to data heterogeneity, system heterogeneity, such as varying computation capabilities, communication latency, and availability, also poses significant challenges to federated learning systems. Partial visibility, a scenario in which only a subset of clients is visible to the server in each communication round, arises from practical considerations

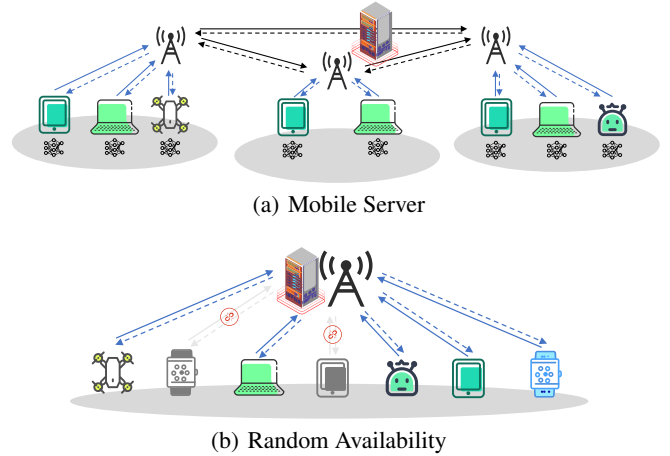


Figure 1: Illustration of 2 representative partial visibility scenarios. 1(a) depicts the scene where the server has to move across different regions; 1(b) depicts the scene where clients intentionally close the connection.

that extend beyond system heterogeneity. In real-world deployments, clients may not always be willing or able to participate in every communication round due to privacy preferences, scheduling constraints, or application-specific policies, leading to dynamically changing and incomplete observations of the client population. Moreover, recent studies, e.g., *Edge-Flow* [Shi *et al.*, 2026], highlight that in large-scale edge networks, the central server itself may need to move across backbone networks to balance connectivity across different network regions. In such scenarios, the server can only interact with clients within its current coverage region. Fig.1 illustrates the two typical source of partial visibility. Motivated by these real-world scenarios, this work aims to enhance the performance of FL under partial visibility.

A substantial body of research has explored a variety of approaches to tackle heterogeneity, among which client selection and aggregation strategies play a central role. Representative existing methods select participating clients based on explicit evaluation metrics (e.g., validation performance or loss reduction), heuristic rules (e.g., resource-aware or fairness-driven criteria), or learning-based policies, including reinforcement learning (RL) formulations. Particularly,

RL-based methods are considered more adaptive and robust against severe heterogeneity. Existing studies, e.g., FAVOR [Wang *et al.*, 2020], FLASH-RL [Bouaziz *et al.*, 2023], FedAgent [Sun *et al.*, 2025], commonly formulated client selection in federated learning under data heterogeneity as a Markov Decision Process (MDP), and have leveraged RL to learn adaptive selection policies. However, these approaches typically rely on the assumption that the server has access to information of the entire client population in every communication round in order to guide the selection process, leaving client selection under partial visibility an under-explored problem that calls for principled modeling and algorithmic solutions.

Inspired by these works, we consider client selection as a sequential decision-making problem, but further accounting for partial visibility. Under this background, we naturally formulate the client selection as a Partially Observable Markov Decision Process (POMDP), since the server’s observations provide incomplete information about the underlying global training state. To make effective decisions in a POMDP, existing theorems and methods incorporate historical information composed of former observations and decisions. Such historical context enables the server to reason about the relationship between the underlying states and the observations, mitigating the uncertainty introduced by partial visibility.

To model the complex dependencies among visible clients and historical information, we introduce the *Attention* mechanism, a widely adopted approach for handling variable-length and sequential inputs while capturing interactions among different entities. Building upon this, we propose a *Spatio-Temporal attention* architecture that integrates historical global information with current observations, enabling solving the POMDP with Deep Q-Learning (DQL).

In this paper, we propose an RL-based client selection framework for federated learning under partial visibility. We formulate the client selection as a POMDP in section 3.2, and propose a DQL solution in section 3.3. The detailed structure of the Spatial-Temporal attention is introduced in section 3.4. Experiments under heterogeneous data distributions demonstrate the effectiveness of the proposed method across different partial visibility settings.

## 2 Related Works

Reinforcement Learning has attracted increasing attention for client selection in federated learning. In this paradigm, client selection is modeled as a policy that interacts with the environment through the aggregated global model. [Wang *et al.*, 2020] proposed FAVOR, which formulated the DQL considering data heterogeneity and selected the clients with the greatest Q values. This work shows the potential of RL in client selection. FLASH-RL [Bouaziz *et al.*, 2023] integrated system heterogeneity, i.e., communication delay, into the DQL-based framework and introduced a reputation-based reward, enabling the server to conduct FL faster. The evaluation of FLASH-RL on different communication channels shows the ability of RL-based client selection to tackle system heterogeneity. FedAgent [Sun *et al.*, 2025] further studies DQL-based client selection. This work addresses the

overestimation of Q values in DQL using a Double Deep Q-network. Knowledge Distillation is integrated to further align the local training of each client. Other RL frameworks are also studied in FL scenarios. [Chen *et al.*, 2024a] leverages an Actor-Critic framework to provide continuous aggregation weights for different participating clients. While these works shaped the paradigm of RL-based client selection, most existing works formulate the state of MDPs as indicators of all clients, relying on full visibility.

The study of partial visibility in FL is inspired by some early works of Decentralized Federated Learning (DFL) [Chang *et al.*, 2018] and Sequential Federated Learning (SFL) [Kopparapu and Lin, 2020]. DFL is a paradigm where clients communicate with each other directly to exchange updated parameters. SFL is a common variant of DFL, where clients update the model in a fixed sequence and pass the update parameters to the next clients. [Yu *et al.*, 2025] proposed Snake Learning, integrating a server with the framework of SFL. The server communicates and exchanges parameters with each client sequentially while leveraging knowledge distillation to update the global model. EdgeFlow [Shi *et al.*, 2026] extends the idea that the server migrates among different edges of a network, having access to a group of clients simultaneously rather than one client at a time. The authors also proved the convergence of the training process and proposed a client selection strategy based on the stochastic gradient of clients.

Since proposed in [Vaswani *et al.*, 2017], *Attention* mechanisms provide a flexible way to model interactions among elements in a set or sequence by dynamically weighting their relative importance. A large body of research leverages attention mechanisms in the client selection scenario. FedABC [Ye *et al.*, 2025] proposed an attention-based algorithm to select clients with relevant semantics and reduce the total selection size. The attention weight is formulated by the KL-divergence across the output distributions of updated parameters, which is deterministic instead of learnable. [Chen *et al.*, 2024b] proposed FedACS, which measures the similarity of clients through the cosine distance of model parameters and constructs the attention weights upon the similarity matrix. FedAWAC [Zhang *et al.*, 2025] studied through the perspective of overcoming catastrophic forgetting in FL, which is a phenomenon where the global model parameters adapt to fresh data and deviate from the global optimum. The updated parameters of different clients are re-weighted based on the variance of output logits. The global parameters are averaged with a window of recent global parameters to avoid forgetting. Training learnable attention networks for client selection remains relatively under-explored, as the server-side lacks sufficient supervised signals and well-defined objectives for neural network optimization. DQL provides a natural solution by enabling training through replay buffers and temporal-difference losses, which is the motivation of this paper.

### 3 Methods

#### 3.1 Problem Formulation

We consider an FL system consisting of a central server and a population of  $N$  clients, denoted as  $\mathcal{U} = \{1, \dots, N\}$ . Each client possesses a local dataset  $\mathcal{D}_n \triangleq \{(\mathbf{x}_i, y_i)\}_{i=1}^{|\mathcal{D}_n|}$ . In conventional FL systems, e.g., FedAVG [McMahan *et al.*, 2017], the goal is to minimize the global objective function:

$$\min_W \left\{ \frac{1}{N} \sum_{n=1}^N \mathbb{E}_{\mathbf{x}, y \in \mathcal{D}_n} [l(\mathbf{x}, y; W)] \right\} \quad (1)$$

where  $W \in \mathbb{R}^{d_{model}}$  denotes the parameters of a neural network, and  $l(\cdot)$  denotes the loss function. In the  $t^{\text{th}}$  communication round, the server select a subset of  $K$  clients, denoted as  $\mathcal{S}^t \subseteq \{1, \dots, N\}$ , and send a copy of the current global parameters  $W_{glob}^t$  to each selected client. The selected clients run *Stochastic Gradient Descent* (SGD) to get the updated parameters  $\{W_i^t\}_{i \in \mathcal{S}^t}$ . The server aggregates the updated parameters according to Eq.2:

$$W_{glob}^{t+1} = \sum_{i \in \mathcal{S}^t} \frac{|\mathcal{D}_i|}{\sum_{j \in \mathcal{S}^t} |\mathcal{D}_j|} \cdot W_i^t \quad (2)$$

Under partial visibility, the client selection during the  $t^{\text{th}}$  communication round is restricted to being sampled from currently visible clients, referred to as a *cluster* in this paper, denoted as  $\mathcal{C}^t \subset \{1, \dots, N\}$ . Therefore, we have the restricted selection range  $\mathcal{S}^t \subseteq \mathcal{C}^t$  where  $\mathcal{C}^t$  is externally determined and may vary across communication rounds, resulting in higher difficulty for a balanced sampling over the entire client population.

#### 3.2 POMDP Model

In this paper, we model the process of client selection and aggregation as a POMDP. A typical POMDP consists of 4 basic elements: *states, actions, rewards, observations*.

##### States

Most existing MDP-based methods define the states as a combination of local model parameters from all clients and a group of meta-information, including computational capabilities, transmission delay, etc. In this paper, we assume the hardware systems are identical among all clients and thus ignore the meta-information, since our research focuses mainly on partial visibility and data heterogeneity.

Therefore, we define the state of the  $t^{\text{th}}$  round as the *potential* updated parameters from every clients:

$$s^t \triangleq (W_1^t, W_1^t, \dots, W_N^t) \quad (3)$$

$$\text{where } W_i^t = W_{glob}^t - lr \cdot \nabla_i W_{glob}^t \quad (4)$$

where  $\nabla_i(\cdot)$  represents the stochastic gradient of the local dataset  $\mathcal{D}_i$  and  $lr$  denotes the learning rate.

It is worth noting that the definition of states serves as a conceptual description. It does not imply that the server has access to the gradients or local updates of invisible clients, nor that such updates are actually computed. The agent only receives the *observations* in a POMDP.

##### Actions

We define the actions as the selected clients' IDs within the current cluster:

$$a^t \triangleq \{a_1^t, a_2^t, \dots, a_K^t\} \subseteq \mathcal{C}^t \quad (5)$$

##### Rewards

The principle of reward design is that the reward directly reflects the performance of the global model after taking an action. In our work, the reward is defined as follows:

$$r^t = \lambda \cdot \mathcal{M}(W_{glob}^{t+1}) + (1 - \lambda) \cdot r^{t-1} \quad (6)$$

where  $\mathcal{M}(\cdot)$  is the F1-score of the global model, which is a widely used metric for reward design in RL-based client selection methods.  $\lambda$  is a hyperparameter to control the variance of the reward.

The F1-score is computed on a small server-side public validation dataset, which is significantly smaller than both the training data and the test set. This setting is commonly adopted in existing federated learning studies [Shi *et al.*, 2026; Bouaziz *et al.*, 2023; Zhang *et al.*, 2025; Chen *et al.*, 2024a; Ye *et al.*, 2025].

##### Observations

Due to partial visibility, the server is unable to collect the entire state  $s^t$ . Instead, it is able to collect a subset of the potential updated parameters, along with the IDs of the visible clients. Therefore, we define the observation for communication round  $t$ :

$$o^t = \{(W_j^t, j)\}, j \in \mathcal{C}^t \quad (7)$$

The observation can be interpreted as the state  $s^t$  masked by the visibility  $\mathcal{C}^t$ . Therefore, the observation function of POMDP is:

$$O(a^{t-1}, s^t, o^t) = \Pr(o^t | a^{t-1}, s^t) = \Pr(\mathcal{C}^t) \quad (8)$$

#### 3.3 Deep Q-Learning (DQL) Solution

In this section, we develop a DQL-based agent to solve the POMDP and make client selection decisions under partial visibility.

Unlike many RL problems, FL is characterized by limited samples and irreversible actions, where model updates cannot be rolled back once applied. Under such constraints, DQL, as an off-policy learning algorithm, is particularly suitable due to its sample efficiency and natural compatibility with discrete decision spaces, making it well aligned with client selection in FL.

##### History-based Q-function Approximation

The canonical approach to POMDP solutions conditions policy decisions upon the cumulative interaction history [Murphy and others, 2000]:

$$h_{1:t} = \{o^1, a^1, o^2, a^2, \dots, o^t\}. \quad (9)$$

However, maintaining the full history is computationally impractical. Instead, we approximate the optimal Q-function using a truncated *temporal context* of the most recent  $H$  rounds:

$$Q(h_{1:t}, a) \approx Q(h_{t-H:t}, a), \quad (10)$$

which is assumed to capture sufficient temporal information.

### Client-wise Q-value Decomposition

At round  $t$ , an action  $a^t$  corresponds to selecting a subset of  $K$  clients from the visible cluster  $\mathcal{C}^t$ . To handle variable cluster sizes and combinatorial action spaces, we decompose the Q-function into client-wise components:

$$Q(h_{t-H:t}, a^t) = \frac{1}{K} \sum_{i=1}^K \hat{Q}(h_{t-H:t}, a_i^t), \quad (11)$$

where  $\hat{Q}(h_{t-H:t}, a_i^t)$  denotes the estimated contribution of selecting client  $a_i^t$  under the current history. This formulation enables the agent to evaluate each visible client independently and select the top- $K$  clients with the highest Q-values, naturally supporting clusters with varying sizes.

### Multi-Step DQN Optimization Objective

The client-wise Q-function  $\hat{Q}(\cdot)$  is parameterized by a deep neural network and trained using multi-step temporal-difference learning. Given a transition sequence of length  $H$  starting from round  $t$ , the multi-step target is defined as:

$$y^t = \sum_{k=0}^{H-1} \gamma^k r^{t+k} + \gamma^H \max_{a' \subseteq \mathcal{C}^{t+H}} Q(h_{t+1:t+H}, a') \quad (12)$$

where  $\gamma \in (0, 1)$  is the discount factor. The corresponding optimization objective is given by:

$$\mathcal{L}_{\text{DQN}} = \mathbb{E} \|y^t - Q(h_{t-T:t}, a^t)\|^2 \quad (13)$$

In practice, the maximization over the action space at round  $t+T$  is efficiently implemented by selecting the top- $K$  clients according to their client-wise Q-values.

### Temporal Parameter Aggregation

Inspired by [Zhang *et al.*, 2025], we average the global parameters over the temporal context window:

$$W_{glob}^{t+1} = \frac{1}{H} \left( \hat{W}_{glob}^{t+1} + \sum_{\tau=0}^{H-2} W_{glob}^{t-\tau} \right) \quad (14)$$

where  $\hat{W}_{glob}^{t+1}$  is obtained by Eq.2.

This operation explicitly incorporate historical information into the global parameters, aligning with the multi-step DQL target  $y^t$  in terms of perceivable history length.

### 3.4 Spatio-Temporal Attention-based Q-Network

This subsection presents our Spatial-Temporal Attentive Q-network, a novel architecture designed to estimate per-client Q-values under partial visibility constraints.

#### Representing Temporal Context

In our POMDP setting, the reward at each communication round is evaluated based on the aggregated global model after the client selection. As a result, the effect of an action is tightly coupled with the aggregated global parameters. To capture such temporal dependencies and strengthen the alignment between the reward signal and the Q-network input, we utilize a sequence of historical global parameters  $[W_{glob}^{t-H}, W_{glob}^{t-H+1}, \dots, W_{glob}^t]$  from the current and the most recent  $H$  communication rounds as temporal context.

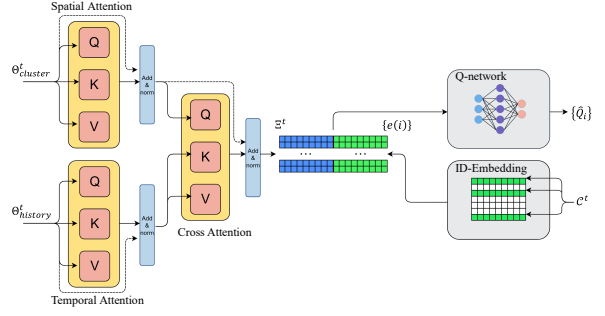


Figure 2: Architecture of the Spatio-Temporal Attention-based Q-Network.

Specifically, the historical global parameters serve as a compact summary of the recent training trajectory, which is more efficient computationally and is supposed to contain all the reward-associated information in  $[o^{t-H}, a^{t-H}, \dots, o^{t-1}, a^{t-1}]$ .

Therefore, the input of the Q-network can be represented by the following tuple:

$$\begin{aligned} \hat{Q}(h_{t-H:t}, a) &\triangleq \hat{Q}(W_{glob}^{t-H:t}, o^t, a) \\ &= \hat{Q}(W_{glob}^{t-H:t}, \{W_i^t\}_{i \in \mathcal{C}^t}, C^t, a) \end{aligned} \quad (15)$$

#### Dimension Reduction of model parameters

Both local and global model parameters are typically high-dimensional, making it computationally expensive to directly apply original parameters as the input to the Q-network.

To obtain compact yet informative representations, we map the original model parameters into a low-dimensional feature space before further processing through Random Projection (RP):

$$\text{RP} : \mathbb{R}^{d_{\text{model}}} \mapsto \mathbb{R}^{d_{\text{feat}}}, \quad \text{RP}(W) = \frac{1}{d_{\text{feat}}} \cdot P \cdot W \quad (16)$$

where  $P \in \mathbb{R}^{d_{\text{feat}} \times d_{\text{model}}}$  is the projection matrix and its elements are independently sampled from the Standard Gaussian Distribution  $\mathcal{N}(0, 1)$ .

A large body of existing works leverage Principal Component Analysis (PCA) as a dimension reduction method [Sun *et al.*, 2025; Wang *et al.*, 2020; Bouaziz *et al.*, 2023]. Under partial visibility, however, the visible clients vary over time, making it uncertain for the server to collect sufficient and representative samples to initiate PCA. In contrast, RP possesses similar properties (linearity, near-orthogonality, etc.) without requiring pre-collecting samples.

#### Spatio-Temporal Attention Architecture

Given a set of queries  $Q$ , a set of keys  $K$ , and values  $V$ , the output of an attention head is defined as:

$$\text{Attn}(Q, K, V) = \text{Softmax} \left( \frac{Q^T \times K}{\sqrt{d_{\text{token}}}} \right) \times V \quad (17)$$

where  $Q, K, V$  are obtained by multiplying the inputs with a learnable matrix respectively.

In our work, each parameter vector of the local updated model  $W_i^t$  is first compressed via RP to get the feature vector  $\omega_i^t$ . We transform the feature vectors into the input tokens of attention heads  $\theta_i^t$  through a lightweight unlinear encoder, denoted as  $f_{\text{enc}}(\cdot) : \mathbb{R}^{d_{\text{feat}}} \mapsto \mathbb{R}^{d_{\text{token}}}$ ,  $\theta_i^t = f_{\text{enc}}(\omega_i^t)$ , in order to rebuild the semantics of the parameters and normalize the scales.

Based on the encoded tokens, we construct a Spatial-Temporal attention architecture to jointly capture inter-client relationships and temporal context. The overall architecture of the network is illustrated in Fig.2.

At each communication round, a *Spatial Attention* module is applied over the set of visible client tokens, allowing the Q-network to reason about the relative contribution of different clients within the same cluster. This Spatial Attention module is inherently invariant to the ordering of the cluster.

To incorporate temporal context, the encoded tokens of the most recent global parameters are processed by a *Temporal Attention* module. This module enables the network to capture temporal dependencies and the relationship between varying rewards and parameter differences. The Temporal Attention module is implemented with Positional Encoding and Casual Mask to learn the order of the tokens.

Finally, the processed spatial and temporal tokens are integrated through cross-attention, where client representations attend to the historical global context. This design allows the Q-network to evaluate each client based on the temporal context, resulting in context-aware client features for subsequent Q-value estimation.

We add residual connection to each attention head for stable gradient back-propagation and consistent latent space. The overall function of attention layers is formulated as:

$$\Xi^t = \Theta_{\text{Spatial}}^t + \text{Attn}(\Theta_{\text{Spatial}}^t, \Theta_{\text{Temporal}}^t, \Theta_{\text{Temporal}}^t) \quad (18)$$

$$\text{where } \Theta_{\text{Spatial}}^t = \Theta_{\text{cluster}}^t + \text{Self-Attn}(\Theta_{\text{cluster}}^t) \quad (19)$$

$$\text{and } \Theta_{\text{Temporal}}^t = \Theta_{\text{history}}^t + \text{Self-Attn}(\Theta_{\text{history}}^t) \quad (20)$$

where the input  $\Theta_{\text{cluster}}^t = [\theta_1^t, \dots, \theta_{|C^t|}^t]$  and  $\Theta_{\text{history}}^t = [\theta_{\text{glob}}^{t-H}, \dots, \theta_{\text{glob}}^t]$ . The function  $\text{Self-Attn}(\cdot)$  equals to  $\text{Attn}(\cdot, \cdot, \cdot)$ .

### Identity-Aware Embedding and Memory

Intermittent client participation under partial visibility induces temporal sparsity in observation trajectories, fundamentally impeding long-term contribution assessment. To overcome this, we propose an Identity-Aware Embedding module that generates unique client fingerprints via trainable identity vectors, enabling cross-round impact modeling despite discontinuous appearances. It is defined as:

$$e(\cdot) : \mathbb{N} \mapsto R^{d_{\text{emb}}} \quad (21)$$

These ID embeddings serve as client-level memory, enabling the Q-network to capture persistent, client-specific characteristics across rounds.

### Dueling Q-Value Decomposition

Finally, the Q-network adopts a dueling architecture to separately estimate the global value of the current training state

| Dataset  | Visibility | Heterogeneity | FedProx    | HA-EdgeFlow | FedAWAC           | Ours              |
|----------|------------|---------------|------------|-------------|-------------------|-------------------|
| CIFAR-10 | MS         | Dirichlet     | 68.28±2.05 | 67.40±0.24  | 72.08±0.78        | <b>76.35±2.88</b> |
|          |            | Label Skew    | 41.86±1.53 | 37.94±2.60  | 42.56±3.76        | <b>50.77±2.33</b> |
|          | RA         | Dirichlet     | 64.48±1.95 | 68.21±1.38  | 74.60±1.83        | <b>74.58±1.42</b> |
| Fashion  | MS         | Dirichlet     | 41.84±2.27 | 43.27±1.13  | 46.24±3.20        | <b>53.07±1.08</b> |
|          |            | Label Skew    | 79.99±0.98 | 81.47±0.52  | 85.27±0.51        | <b>85.96±0.31</b> |
|          | RA         | Dirichlet     | 63.34±2.44 | 59.05±0.80  | 60.19±3.53        | <b>68.71±1.98</b> |
| UCI-HAR  | MS         | Dirichlet     | 79.26±0.39 | 81.33±2.40  | <b>85.67±0.45</b> | 85.68±1.01        |
|          |            | Label Skew    | 61.17±1.46 | 52.00±0.31  | 63.11±0.05        | <b>73.35±0.31</b> |
|          | RA         | Dirichlet     | 92.48±0.50 | 90.00±0.44  | <b>92.53±0.42</b> | 91.53±0.40        |
|          |            |               | 91.94±0.91 | 91.26±0.25  | <b>93.02±0.87</b> | 91.54±0.51        |

Table 1: Test Accuracy (mean±std) of different methods on different settings. The table reports the average accuracy of the last 10 communication rounds to mitigate the influence of fluctuation. The mean and std are obtained from 3 independent runs with different RA seeds.

and the relative advantage of selecting each client:

$$\hat{Q}_i^t = \text{Val}(\bar{\xi}^t, \bar{e}) + \text{Adv}(\xi_i^t, e(i)) - \bar{Adv} \quad (22)$$

where  $\xi_i^t$  denotes the  $i^{\text{th}}$  vector of  $\Xi^t$ , and variables with a bar denotes the average over  $i \in C^t$ .

## 4 Experimental Analysis

### 4.1 Datasets

We conduct experiments on three representative datasets, including:

- **CIFAR-10**: A standard image classification dataset containing 60,000 RGB images in 10 classes, with 50,000 training images and 10,000 test images.
- **Fashion-MNIST**: A dataset of grayscale images, consisting of 60,000 training images and 10,000 test images across 10 fashion categories.
- **UCI-HAR** [Reyes-Ortiz *et al.*, 2013]: A dataset of accelerometer signals collected from smartphones of 30 subjects. The target is to detect human activities, e.g., walking&sitting.

### 4.2 Data Heterogeneity Simulation

To evaluate the robustness of our method against severe data heterogeneity, we construct the non-IID distributions of local datasets with the following strategies:

- **Dirichlet Distribution**: A widely used non-IID setting, partitioning the datasets among clients using a Dirichlet distribution with concentration parameter  $\alpha$ . We set  $\alpha = 0.1$  in our experiments to create heterogeneous distributions.
- **Label Skew Distribution**: We assign each client a subset of classes, ensuring that each client only has data from 2 number of classes. This simulates scenarios where each client has access to extremely limited types of data.

### 4.3 Partial Visibility Settings

To simulate real-world partial visibility scenarios, we design two visibility patterns:

- **Mobile Server (MS)**: Server moves across different network regions (Fig.1(a)). Clients are grouped into clusters, and the server randomly connects to one of the clusters at each communication round.

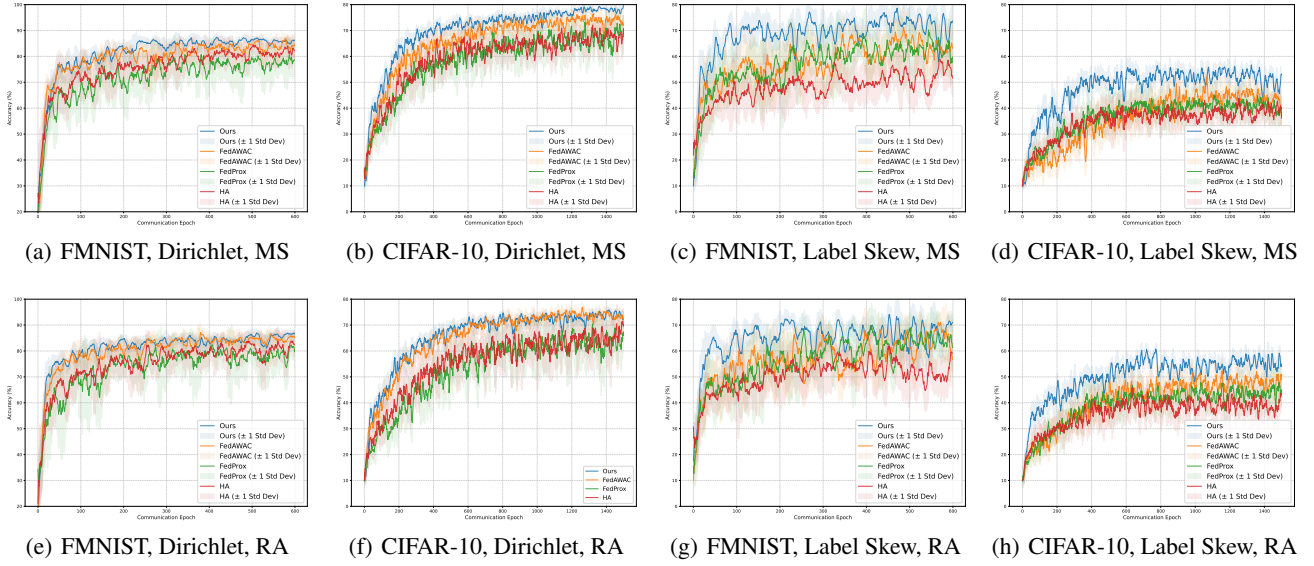


Figure 3: Accuracy versus Communication epochs under various settings. The curves are smoothed using a moving average with a window size of 10 for better readability, and the shaded regions indicate the standard deviation within the moving window.

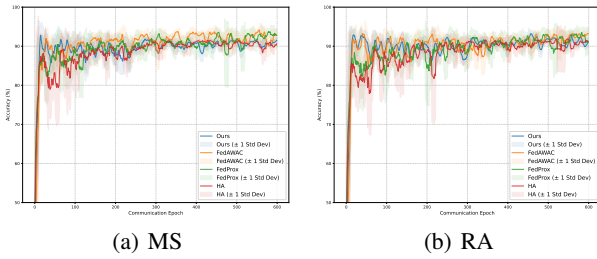


Figure 4: Accuracy versus Communication epochs on UCI-HAR.

- **Random Availability (RA):** All clients have an identical probability  $p$  of being available at each communication round (Fig.1(b)). The selection size is  $\min(|\mathcal{C}^t|, K)$  under this setting.

#### 4.4 Baselines

We compare our method with the following baselines:

- **FedProx** [Li *et al.*, 2020] : A widely used federated learning algorithm that introduces a proximal term to the local objective to mitigate the impact of data heterogeneity.
- **HA-EdgeFlow** [Shi *et al.*, 2026] : A method designed for federated learning with a mobile server, which selects clients based on the norm of gradient differences. We use the implementation provided by the Shi *et al.*<sup>1</sup>.
- **FedAWAC** [Zhang *et al.*, 2025] : A method designed for overcoming catastrophic forgetting in FL, which assigns different weights to clients based on the variance of the

logits predicted by local models and averages the global models of recent communication rounds for aggregation.

#### 4.5 Implementation Details

All experiments are implemented in PyTorch 2.4.0. For the CIFAR-10 and Fashion-MNIST datasets, we set  $N = 100$ , and each client has the same size of local dataset. For the UCI-HAR dataset, we consider each subject as a client so that  $N = 21$  and the local data is naturally non-IID. Each selected client performs local training using SGD with a learning rate of 0.001 and a batch size of 64 for 3 local epochs. For the DQN agent, the transitions are cached in a replay buffer with a length of 600. The discount factor  $\gamma = 0.9$ . We adopt the Double-DQN strategy, where the soft-update rate is set to 0.005. Unless otherwise specified, models are trained for 1500 communication rounds on CIFAR-10 and 600 rounds on Fashion-MNIST, with the client selection size  $K$  fixed to 5 by default. In the Mobile Server scenario, each cluster contains 10 clients, while in the Random Availability scenario, each client is visible with a probability of  $p = 0.1$ .

#### 4.6 Accuracy Performance

Under identical partial visibility settings, we benchmark our method against state-of-the-art baselines.

As quantified in Table 1, our proposed method achieves superior accuracy across nearly all evaluated scenarios, while demonstrating relatively low standard deviations over multiple runs, confirming its enhanced robustness. Our method enhances the average accuracy over all settings by 3.6 ~ 7.9% compared to the baselines.

Fig.3 demonstrates the accuracy evolution of different methods under various partial visibility and heterogeneity settings. Under identical heterogeneity, the accuracy evolution trend of each method remains consistent across both visibility scenarios. Our proposed method demonstrates substantial

<sup>1</sup><https://github.com/hqj-les30/HA-EdgeFlow>

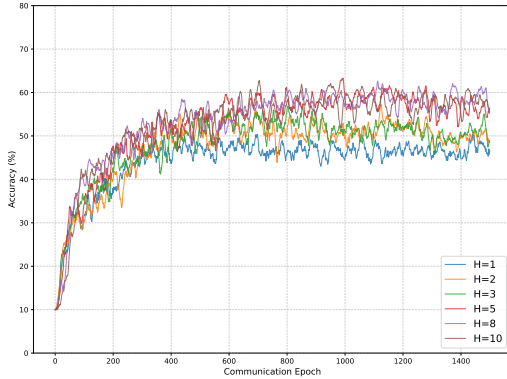


Figure 5: Accuracy versus Communication epochs for different  $H$

performance gap over the baselines in the Label Skew scenarios (Fig.3(c)(d),(g)(h)), characterized by both faster accuracy increasing and superior accuracy after convergence. Under Dirichlet distribution, although the accuracy difference among methods is relatively moderate, our method still outperforms the baselines. Notably, our method also shows reduced performance fluctuations after convergence, as evidenced by the narrower shadow regions, indicating improved stability (Fig.3(a)(b),(e)(f)). In addition, the performance gains of our method are more pronounced in the Mobile Server scenario compared to the Random Availability.

Fig.4 illustrates the accuracy on the UCI-HAR dataset, where data heterogeneity across clients is not as severe as the Dirichlet and Label Skew distributions. In this case, all methods achieve final accuracy over 90%. Our method still significantly reduces the fluctuations. In summary, in challenging scenarios where all methods exhibit relatively low accuracy, our approach tends to enhance accuracy. Conversely, when all methods achieve relatively high accuracy, our method reduces fluctuations and enhance training stability.

#### 4.7 Impact of Context Length $H$

In this subsection, we investigate the impact of the length  $H$  of temporal context, defined in Eq.11. Since we formulate the client selection problem as a POMDP and introduce temporal context as a solution, the impact of  $H$  validates the necessity of our formulation. Notably, the POMDP-based solution degenerated to an MDP-based solution when  $H = 1$ , since the decision no longer relies on the context. Fig.5 demonstrates the accuracy versus communication rounds of various  $H$  on CIFAR-10 dataset under Mobile-Server-style partial visibility and Label Skew distribution. Similar trends are observed under other settings and thus omitted for brevity.

As illustrated in Fig.5, the MDP-based case ( $H = 1$ ) yields the lowest performance, confirming that the MDP-based solution is less suitable for the partial visibility scenario compared to POMDP. The performance improves as  $H$  increases up to 5, indicating that incorporating additional historical information enhances the model selection process. However, further enlarging the context length to  $H = 8, 10, 12$  brings no noticeable performance improvement. This suggests that recent states and actions of the FL server already contain sufficient

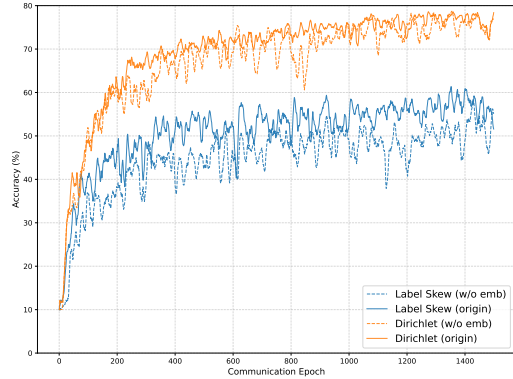


Figure 6: Accuracy versus Communication epochs. *w/o emb* represents the Identity-Aware embedding module is removed.

historical information for effective client selection.

This experiment validates our approach of introducing historical information to address the POMDP. Moreover, we confirm that approximating the full history with a limited-length temporal window is both effective and efficient.

#### 4.8 Ablation Study: Identity-Aware Embedding

In this subsection, we run an ablation experiment to validate the function of the Identity-Aware Embedding module of the Q-network. As shown in Fig.6, under Label Skew distributions, the absence of Identity-Aware embedding results in a noticeable drop in overall accuracy, while the fluctuation remains at a similar level. In contrast, under the Dirichlet distribution, the final accuracy is largely preserved, but the fluctuation significantly increases, indicating a less stable training process.

This phenomenon suggests that under the more challenging Label Skew distribution, where the reward is relatively low, Identity-Aware embedding enables the server to memorize clients that yield high accuracy. Under the Dirichlet distribution, where the reward is relatively high, the server tends to avoid severe degradation.

This experiment demonstrates the effect of the Identity-Aware embedding module we proposed in the Q-network.

## 5 Conclusion

This work established a Partially Observable Markov Decision Process (POMDP) framework for federated client selection under partial visibility. We formulated the POMDP elements and developed a multi-step deep Q-learning (DQL) solution, integrating a Spatial-Temporal Attention Network to encode historical states and dynamically handle variable-length inputs. Extensive experiments across diverse visibility regimes and data heterogeneity levels demonstrated our method’s capacity to enhance final accuracy by 3.6 ~ 7.9%, accelerate convergence, and reduce performance fluctuation. Ablation studies on context length and Identity-Aware embeddings further validated the Spatial-Temporal Attention architecture’s theoretical foundations.

## References

- [Bouaziz *et al.*, 2023] Sofiane Bouaziz, Hadjer Benmezziane, Youcef Imine, Leila Hamdad, Smail Niar, and Hamza Ouarnoughi. FLASH-RL: Federated Learning Addressing System and Static Heterogeneity using Reinforcement Learning. In *2023 IEEE 41st International Conference on Computer Design (ICCD)*, pages 444–447, November 2023. ISSN: 2576-6996.
- [Chang *et al.*, 2018] Ken Chang, Niranjana Balachandar, Carson Lam, Darvin Yi, James Brown, Andrew Beers, Bruce Rosen, Daniel L Rubin, and Jayashree Kalpathy-Cramer. Distributed deep learning networks among institutions for medical imaging. *Journal of the American Medical Informatics Association*, 25(8):945–954, 2018.
- [Chen *et al.*, 2024a] Leiming Chen, Weishan Zhang, Cihao Dong, Sibao Qiao, Ziling Huang, Yuming Nie, Zhaoxiang Hou, and Chee Wei Tan. Feddrl: A trustworthy federated learning model fusion method based on staged reinforcement learning, 2024.
- [Chen *et al.*, 2024b] Zihan Chen, Jundong Li, and Cong Shen. Personalized federated learning with attention-based client selection. In *ICASSP 2024-2024 IEEE International Conference on Acoustics, Speech and Signal Processing (ICASSP)*, pages 6930–6934. IEEE, 2024.
- [Kopparapu and Lin, 2020] Kavya Kopparapu and Eric Lin. Fedfmc: Sequential efficient federated learning on non-iid data. *arXiv preprint arXiv:2006.10937*, 2020.
- [Li *et al.*, 2020] Tian Li, Anit Kumar Sahu, Manzil Zaheer, Maziar Sanjabi, Ameet Talwalkar, and Virginia Smith. Federated optimization in heterogeneous networks. *Proceedings of Machine Learning and Systems*, 2:429–450, 2020.
- [McMahan *et al.*, 2017] Brendan McMahan, Eider Moore, Daniel Ramage, Seth Hampson, and Blaise Agüera y Arcas. Communication-efficient learning of deep networks from decentralized data. In *Artificial intelligence and statistics*, pages 1273–1282. PMLR, 2017.
- [Murphy and others, 2000] Kevin P Murphy *et al.* A survey of pomdp solution techniques. *environment*, 2(10):1–12, 2000.
- [Reyes-Ortiz *et al.*, 2013] Jorge Reyes-Ortiz, Davide Anguita, Alessandro Ghio, Luca Oneto, and Xavier Parra. Human activity recognition using smartphones. UCI Machine Learning Repository, 2013. DOI: 10.24432/C54S4K.
- [Shi *et al.*, 2026] Yuchen Shi, Qijun Hou, Pingyi Fan, and Khaled B. Letaief. Edgeflow: Serverless federated learning via sequential model migration in edge networks, 2026.
- [Sun *et al.*, 2025] Bingli Sun, Xiao Song, Yuchun Tu, and Ming Liu. FedAgent: Federated Learning on Non-IID Data via Reinforcement Learning and Knowledge Distillation. *Expert Systems with Applications*, 285:127973, August 2025.
- [Vaswani *et al.*, 2017] Ashish Vaswani, Noam Shazeer, Niki Parmar, Jakob Uszkoreit, Llion Jones, Aidan N Gomez, Łukasz Kaiser, and Illia Polosukhin. Attention is all you need. *Advances in neural information processing systems*, 30, 2017.
- [Wang *et al.*, 2020] Hao Wang, Zakhary Kaplan, Di Niu, and Baochun Li. Optimizing federated learning on non-iid data with reinforcement learning. In *IEEE INFOCOM 2020 - IEEE Conference on Computer Communications*, pages 1698–1707, 2020.
- [Ye *et al.*, 2025] Wenxuan Ye, Xueli An, Junfan Wang, Xueqiang Yan, and Georg Carle. Fedabc: Attention-based client selection for federated learning with long-term view. In *ICC 2025-IEEE International Conference on Communications*, pages 801–806. IEEE, 2025.
- [Yu *et al.*, 2025] Xiaoxue Yu, Xingfu Yi, Rongpeng Li, Fei Wang, Chenghui Peng, Zhifeng Zhao, and Honggang Zhang. Snake learning: A communication-and computation-efficient distributed learning framework for 6g. *IEEE Communications Magazine*, 2025.
- [Zhang *et al.*, 2025] Benteng Zhang, Yingchi Mao, Haowen Xu, Yihan Chen, Tasiu Muazu, Xiaoming He, and Jie Wu. Overcoming Forgetting Using Adaptive Federated Learning for IIoT Devices With Non-IID Data. *IEEE Internet of Things Journal*, pages 1–1, 2025. Conference Name: IEEE Internet of Things Journal.